

Modelling and Simulation of Hydrogen Production via Water Gas Shift Membrane Reactor

Aya Abdel-Hamid I. Mourad, Nayef Mohamed Ghasem, and Abdulrahman Yaqoub Alraeesi

Abstract—A simulation study of a double tubular catalytic membrane reactor for the water–gas shift (WGS) reaction under steady-state operation is presented. The membrane consists of dense Pd layer deposited on a porous glass cylinder support. The WGS model was carried out with and without the membrane at a temperature of 673 K, pressure of 2atm, argon flow rate of $400 \text{ cm}^3 \cdot \text{min}^{-1}$, and steam-to-carbon (S/C) ratio of 1. The membrane reactor could achieve a Carbon Monoxide (CO) conversion efficiency of up to 93.7%, whereas a maximum value of only 77.5% was attained without using a membrane. In order to find the optimum operating conditions, the response surface method was used. It was found that a nearly complete CO conversion could be achieved at S/C ratio = 4, total retentate pressure =12 atm, and membrane thickness =5 μm . There is a good agreement between the model results and the reported experimental results.

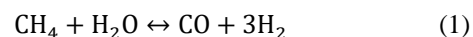
Index Terms—Membrane reactor, Palladium (Pd) composite membrane, water–gas shift reaction (WGSR), response surface method (RSM).

I. INTRODUCTION

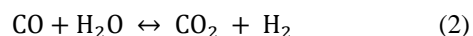
The increasing demand for energy, diminishing worldwide petroleum reserves, high petroleum prices, and high environmental standards for clean fuels have incentivised consistent efforts for developing new and alternative energy sources [1]. The production of hydrogen has become an important topic in recent decades; however, it is currently of greater interest because of fuel-cell technological developments [2]. Fuel cells that use H_2 as an energy source are environmentally friendly as compared to the traditional forms of combustion using fuels such as gasoline and diesel, in the sense that the only by-product from H_2 fuel cells is water, and therefore, it eliminates the emission of greenhouse gases [3]. In addition, hydrogen is used in the production of certain chemical products, particularly methanol, and for ammoniac synthesis [4]. Furthermore, hydrogen is used in a range of other industries, including metal refining, food processing, and electronics manufacturing [5].

The steam reforming (SR) of methane is currently the most cost-effective and highly developed method for the production of hydrogen, with a relatively low cost and high hydrogen-to-carbon ratios that are desired for hydrogen production [6]. The entire process is comprised of two main stages [7]. In the first stage, methane is mixed with steam and fed into a tubular catalytic reactor. During this process,

syngas (H_2/CO gas mixture) is produced, as shown in (1) [8].



In the second stage, CO is converted to H_2 and CO_2 according to the water–gas shift (WGS) provided by (2).



The purpose of the water–gas shift reaction (WGSR) is to reduce the CO production and to optimise the production of hydrogen. The WGSR is limited by the thermodynamic equilibrium at low temperatures; however, high temperatures are required to ensure the necessary reaction rates. In order to take advantage of both the thermodynamics and kinetics of the reaction, the WGSR is carried out in two stages. A high-temperature reaction stage operated at approximately 593–723 K with the use of $\text{Fe}_3\text{O}_4/\text{Cr}_2\text{O}_3$ catalyst [9], [10] and a low-temperature reaction stage operated at approximately 473–523 K using $\text{Cu}/\text{ZnO}/\text{Al}_2\text{O}_3$ catalysts [9]–[11]. Iron- and copper-based catalysts are commonly used in industry for the high- and low-temperature stages, respectively [12]. The product mixture from the WSGR (CO , H_2 , H_2O , and CO_2) is then passed either through a CO_2 -removal and methanation, or through a pressure swing adsorption (PSA), leaving H_2 with a high purity of near 100% [13]. PSA is the most widely used technology for hydrogen purification [14].

Both the WGSR processes and the CO_2/H_2 separation process can be combined in a single catalytic membrane reactor (CMR) using a high-temperature WGS catalyst to achieve CO conversion levels higher than that of the two-step WGS reactor configuration. This is explained by the continuous removal of one of the reaction products through the selective membrane, which drives the equilibrium of the WGSR to the right [15]. If the membrane is H_2 -selective, the product streams would consist of a low-pressure, high-purity H_2 stream and a high-pressure CO_2 -steam stream [9].

In this work, a 2D-axisymmetric MR model was developed to achieve a better understanding and optimization of the MR performance under different operating conditions. One of the main objectives of this reactor-optimization task is to run the MR within a targeted range of operating conditions to achieve the highest possible CO conversion.

II. MODEL DEVELOPMENT

The model was developed to predict the experimental data for experiments conducted at 673 K in a double-tubular-type reactor with an iron-chromium oxide catalyst, which has been described elsewhere [16]. Briefly, the inner tube was fabricated from a palladium membrane with an outer

Manuscript received June 10, 2018; August 16, 2018.

Aya Abdel-Hamid I. Mourad is with the Academic Support Department, Abu Dhabi Polytechnic, Institute of Applied Technology, P.O. 111499, Abu Dhabi, United Arab Emirates (e-mail: Aya.abdelhamid@adpoly.ac.ae).

N. M. Ghasem and A. Y. Alraeesi are with Department of Chemical and Petroleum Engineering, Faculty of Engineering, United Arab Emirates University, P.O. 15551, Al-Ain, United Arab Emirates (e-mail: nayef@uaeu.ac.ae, a.alraeesi@uaeu.ac.ae).

diameter of 10 mm and the outer tube was made from a quartz tube with an inner diameter of 18 mm. The palladium membrane was of a composite structure consisting of a thin palladium film with a thickness of 20 μm supported on the outer surface of a porous-glass cylinder (mean pore size of 300 nm). The use of supported precious metal is preferred because of the high hydrogen flux requirement, which cannot be attained with most currently available dense metal membranes owing to their thickness. The active surface area of the palladium membrane for hydrogen separation was 25.1 cm^2 . The annular space surrounding the membrane (reaction side) was filled with a commercial iron-chromium oxide catalyst, designed as Girdler G-3. The mass of the catalyst was 12.1 g and the height of the catalyst bed was 8 cm [17].

A. Model Configuration

The reactor geometry was constructed for a 2D-axisymmetric model using two software packages COMSOL and MATLAB to understand the function of the palladium membrane reactor. The model of the flow in the palladium membrane reactor is presented in Fig. 1. The reactants flow in from the bottom of the reactor and after the catalytic reaction the products flow out of the top. The driving force for hydrogen transportation through a membrane is the hydrogen partial pressure difference between the two surfaces of the palladium membrane. The membrane is selectively permeable to H_2 , allowing H_2 to diffuse out of the reaction zone through the membrane walls, while being impermeable to the other components. A sweep gas, argon (Ar), was concurrently supplied to the permeation side to sweep the permeated hydrogen [17].

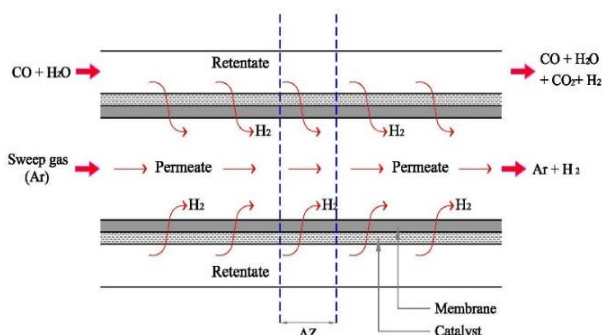


Fig. 1. Schematic representation of gas flow model through reaction and permeation sides in palladium membrane reactor.

B. Model Assumptions

The following assumptions were used in the modelling of the 2D catalyst membrane reactor [17]:

- 1) The membrane reactor was assumed to operate in a steady state.
- 2) An isothermal environment was assumed.
- 3) The pressure drop was assumed to be negligible along the length of the membrane unit.
- 4) The flow was assumed to be a plug flow.
- 5) Complete selectivity of the Pd membrane reactor to H_2 was assumed.
- 6) The rate of hydrogen permeation was assumed to be unaffected by any of the coexisting gases and the reaction occurred only on the iron-chromium oxide catalyst, not on the palladium membrane.

III. MATHEMATICAL MODEL

A. Governing Equation Used in Retentate Side

The mass balances describing the transport and reactions in the retentate side are given by diffusion-convection equation at steady state [17]:

$$D_i \left[\frac{\partial^2 c_i}{\partial r^2} + \frac{1}{r} \frac{\partial c_i}{\partial r} + \frac{1}{r^2} \frac{\partial^2 c_i}{\partial \theta^2} + \frac{\partial^2 c_i}{\partial z^2} \right] + \left[v_r \frac{\partial c_i}{\partial r} + \frac{v_\theta}{r} \frac{\partial c_i}{\partial \theta} + v_z \frac{\partial c_i}{\partial z} \right] = \mathcal{R} \quad (3)$$

where D_i is the inter-diffusion coefficient of species i , c_i is the species concentration, and V is the superficial velocity. The term \mathcal{R} corresponds to the reaction rate expression.

Under the plug flow assumption, the molecular diffusion term is cancelled from (3):

$$\left[v_r \frac{\partial c_i}{\partial r} + \frac{v_\theta}{r} \frac{\partial c_i}{\partial \theta} + v_z \frac{\partial c_i}{\partial z} \right] = \mathcal{R} \quad (4)$$

$$\text{Molar flow rate } (F_i) = V c_i \quad (5)$$

$$\text{Thus, } \left[\frac{\partial F_i}{\partial r} + \frac{1}{r} \frac{\partial F_i}{\partial \theta} + \frac{\partial F_i}{\partial z} \right] = \mathcal{R} \quad (6)$$

Mass balance for the CO component:

$$\left[\frac{\partial F_{\text{CO}}}{\partial r} + \frac{1}{r} \frac{\partial F_{\text{CO}}}{\partial \theta} + \frac{\partial F_{\text{CO}}}{\partial z} \right] = -\mathcal{R} \quad (7)$$

Mass balance for the H_2O component:

$$\left[\frac{\partial F_{\text{H}_2\text{O}}}{\partial r} + \frac{1}{r} \frac{\partial F_{\text{H}_2\text{O}}}{\partial \theta} + \frac{\partial F_{\text{H}_2\text{O}}}{\partial z} \right] = -\mathcal{R} \quad (8)$$

Mass balance for the CO_2 component:

$$\left[\frac{\partial F_{\text{CO}_2}}{\partial r} + \frac{1}{r} \frac{\partial F_{\text{CO}_2}}{\partial \theta} + \frac{\partial F_{\text{CO}_2}}{\partial z} \right] = \mathcal{R} \quad (9)$$

Mass balance for the H_2 component:

For H_2 , the flux term is considered in the equation, because part of the hydrogen is diffused across the membrane and the rest flows out from the retentate side.

$$\left[\frac{\partial F_{\text{H}_2}}{\partial r} + \frac{1}{r} \frac{\partial F_{\text{H}_2}}{\partial \theta} + \frac{\partial F_{\text{H}_2}}{\partial z} \right] = \mathcal{R} - J \quad (10)$$

The mechanism of H_2 permeation through Pd-based membranes has been investigated by many researchers. It has been found that H_2 permeates through the membrane via a solution-diffusion mechanism [18]-[19].

It was observed by Uemiyama *et al.* [16] that the rate of hydrogen permeation per unit length of catalyst bed through the membrane J_{H_2} (mol/cm \cdot min) is correlated to a hydrogen pressure order of 0.76.

$$J_{\text{H}_2} = \frac{q}{t} \left[c_{\text{H}_2,\text{ret}}^{0.76} - c_{\text{H}_2,\text{perm}}^{0.76} \right] \quad (11)$$

where t is the membrane thickness, hydrogen permeation coefficient per unit length of catalyst bed (q) = 1.1×10^2 (mol $^{0.24} \cdot \mu\text{m} \cdot \text{cm}^{2.28}$) / (min \cdot cm reactor length), and $c_{\text{H}_2,\text{ret}}$ and $c_{\text{H}_2,\text{perm}}$ are the concentrations of hydrogen in the retentate and permeate sides, respectively.

The rate equation \mathcal{R} (cm 3 /cm \cdot min) at 673 K is determined

by Uemiya *et al.* [16] as follows:

$$\mathcal{R} = k \frac{c_{\text{CO}} c_{\text{H}_2\text{O}} - K_p^{-1} c_{\text{CO}_2} c_{\text{H}_2}}{1 + 2.4 \times 10^5 c_{\text{H}_2\text{O}} + 7.2 \times 10^5 c_{\text{CO}_2}} \quad (12)$$

where equilibrium constant (K_p) = 11.92 (dimensionless) and reaction rate constant (k) = 7.4×10^8 (cm⁶)/(mol.min.cm reactor length) at 673 K.

B. Governing Equation Used in Permeate Side

Mass balance for the H₂ component:

$$\left[\frac{\partial F_{\text{H}_2}}{\partial r} + \frac{1}{r} \frac{\partial F_{\text{H}_2}}{\partial \theta} + \frac{\partial F_{\text{H}_2}}{\partial z} \right] = J \quad (13)$$

Mass balance for the argon component:

$$\left[\frac{\partial F_{\text{Ar}}}{\partial r} + \frac{1}{r} \frac{\partial F_{\text{Ar}}}{\partial \theta} + \frac{\partial F_{\text{Ar}}}{\partial z} \right] = 0 \quad (14)$$

IV. RESULTS AND DISCUSSION

A. Effect of Using Membrane on CO Conversion

The hydrogen surface plot concentration generated by COMSOL Multiphysics software package is depicted in Fig. 2. The figure illustrates the impact of using the membrane on the WGS species, at temperature of 673 K, retentate pressure of 2 atm, argon flow rate of 400 cm³.min⁻¹ and steam to ratio of 1. The hydrogen concentration increases along the membrane reactor due to increase in reaction rate and the continuous production rate of hydrogen. After certain length in the reactor, the concentration of the hydrogen is reduced in the reaction side because the high diffusivity of hydrogen through the permeable membrane. The hydrogen gas permeated through the palladium membrane to the shell side is continuously swept by argon gas to maintain its concentration to minimum and to maintain the highest possible concentration gradient and hence continues permeation of hydrogen and hereafter the increase in CO conversion. The arrows display the hydrogen permeation pathway, from the retentate side through the membrane to permeate side [17].

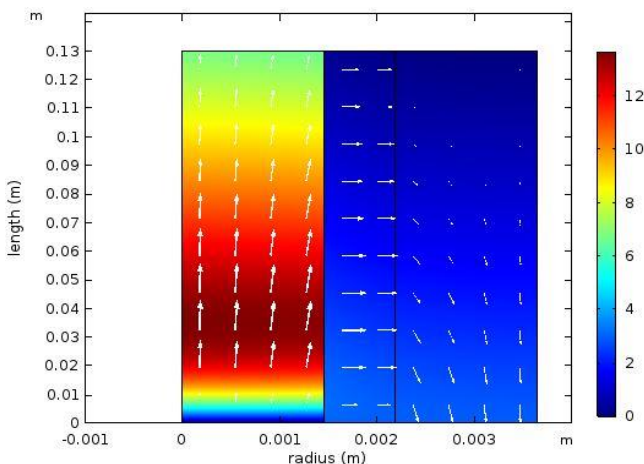


Fig. 2. Surface plot for the hydrogen concentration (mol.m⁻³) in the present of palladium membrane.

Fig. 3 compares the conversion of CO with and without the membrane. As might be expected, it is very clear from the data that the CO conversion of the membrane reactor is

higher than that of the non-membrane reactor. As shown from the figure, the highest conversion reached by using the membrane is 93.7% compared with only 77.5% for the non-membrane reactor. The enhancement in the CO conversion is due to the improvement in hydrogen selectivity through the membrane. The membrane continuously removed the produced H₂ from the reaction zone and therefore increased the driving force across the membrane, shifting the chemical equilibrium towards the products side [17].

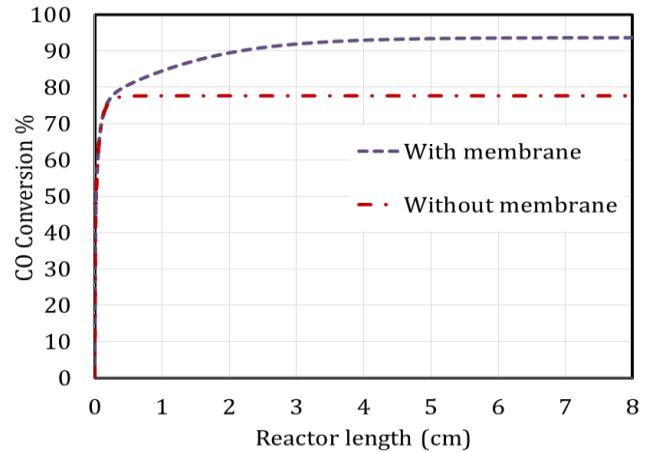


Fig. 3. Change in CO conversion with and without the membrane along the reactor length.

B. Effect of Steam to Carbon Ratio (S/C)

Fig. 4 demonstrates the change in CO conversion at different S/C ratios along the length of the reactor. The effect was examined under a temperature of 673 K, retentate pressure of 2 atm, and sweep argon flow rate of 400 cm³.min⁻¹. As an overall trend, CO conversion increases by increasing the S/C ratio. In addition, it can be observed that the CO conversion is almost the same for the S/C ratios of 4, 5, and 6. This means that increasing the S/C ratio beyond 4 did not significantly affect the change in CO conversion [17].

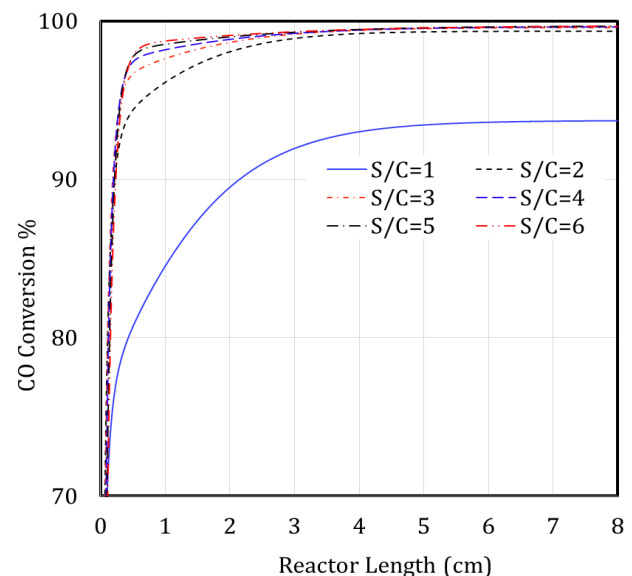


Fig. 4. Change in CO conversion at different S/C ratios.

C. Model Validation

Fig. 5 demonstrates the effect of the S/C molar ratio on the

total CO conversion. The effect was tested by varying the S/C ratio from 1 to 6 at a fixed temperature of 673 K, retentate pressure of 2 atm, and sweep argon flow rate of 400 $\text{cm}^3 \cdot \text{min}^{-1}$. The figure illustrates an enhancing effect of increasing the steam-to-CO ratio on the CO conversion for the Pd membrane reactor. As shown in the figure, an optimum value of the S/C ratio must be employed. The maximum of total methane conversion was obtained for S/C ratio of 4 [17].

To validate the model prediction, the simulation results were compared with the experimental data of Uemiya *et al.* [16], as shown in Fig. 5. The figure shows that the model predictions are in good agreement with the experimental data.

A S/C of 4 is favourable, as it means the energy penalty associated with steam generation is reduced. Additionally, carbon formation can be avoided. Therefore, this value is an intermediate value of the S/C ratio.

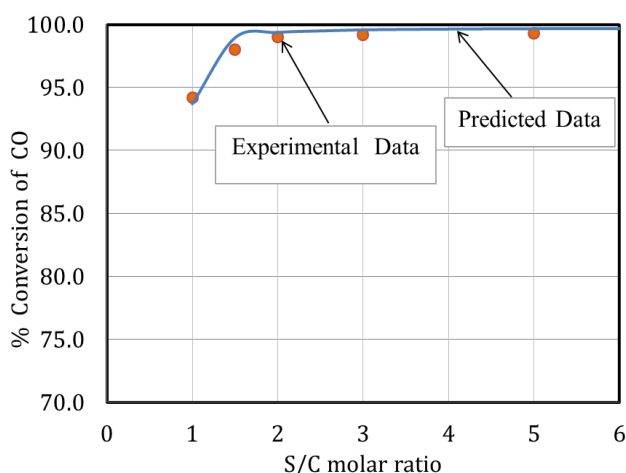


Fig. 5. Effect of S/C molar ratio on CO conversion. Experimental conditions: temperature, 673 K; retentate pressure, 2 atm; flow rate of sweep argon, 400 $\text{cm}^3 \cdot \text{min}^{-1}$.

D. Effect of Membrane Thickness and Sweep Gas Flowrate

The effect of membrane thickness on the total CO conversion was investigated with a computer simulation, as illustrated in Fig. 6, for a temperature of 673 K, a retentate pressure of 2 atm, argon flow rates of 3200, 400, and 100 cm^3/min , and S/C ratio of 1. At first glance, we see that as the membrane thickness decreases, the total conversion increases because of the enhancement in hydrogen removal [17].

As the argon flow rate increases, the partial pressure of hydrogen on the permeation side declines, and therefore, the level of CO conversion increases. At an argon flow rate of 3200 cm^3/min , the CO conversion is approximately 98% at a thickness of 5 μm ; however, at argon flow rates of 400 and 100 cm^3/min , the CO conversion are approximately 93.7% and 87.8%, respectively.

Another aspect which stands out in this graph is that a complete conversion of CO is not reached, but it could be attained if the partial pressure of hydrogen on the permeation side were further decreased by using a higher argon flow rate or by using a vacuum pump that could minimize the hydrogen pressure.

In summary, a membrane reactor constructed with composite palladium membrane gives a significantly high reaction efficiency associated with its excellent hydrogen

permeation performance.

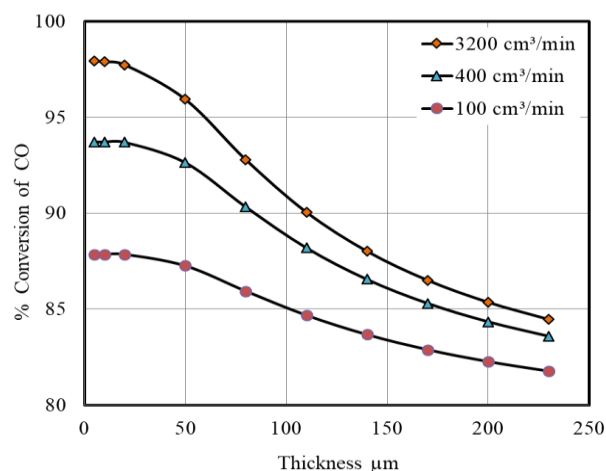


Fig. 6. Effect of thickness on CO conversion for constant CO feed rate of 25 cm^3/min and argon flow rates of 3200, 400, and 100 cm^3/min .

E. Effect of Residence Time

In order to determine the effect of the residence time on the concentrations of the WGS components, the residence times of the reactor systems were varied by changing the operating pressure, while keeping the inlet feed flow rate and reaction temperature constant. This process resulted in a reduced reactant volumetric flow rate and therefore increased the residence time at the elevated pressure conditions inside the reaction zone. The retentate pressures used in the simulation corresponding to the different residence times are listed in Table I. The effect of residence time was examined under a temperature of 673 K, CO inlet volumetric flow rate of 100 cm^3/min , S/C ratio of 1, and sweep argon flow rate of 400 cm^3/min [17].

TABLE I: RETENTATE PRESSURE AND ITS CORRESPONDING RESIDENCE TIME.

Retentate pressure (atm)	Residence time τ (s)
2	0.13
4	0.30
6	0.47
8	0.63
10	0.79
12	0.96
14	1.12

Fig. 7 shows the effect of residence time on CO conversion along the length of the reactor while Fig. 8 depicts the overall CO conversion for each residence time. The impact of residence time was tested under a temperature of 673 K, S/C ratio of 1, CO flow rate of 100 cm^3/min , and argon flow rate of 400 cm^3/min . The figures illustrate an enhancing effect of increasing residence time on CO conversion. It can be noticed that by increasing the residence time from 0.13 to 0.96 s, CO conversion increases from 89.4% to 97.3%. This is due to the same reasons explained above. By increasing the reaction

pressure, the residence time increased and the driving force across membrane increased as well. Therefore, hydrogen permeability went up and rate of reaction increased [17].

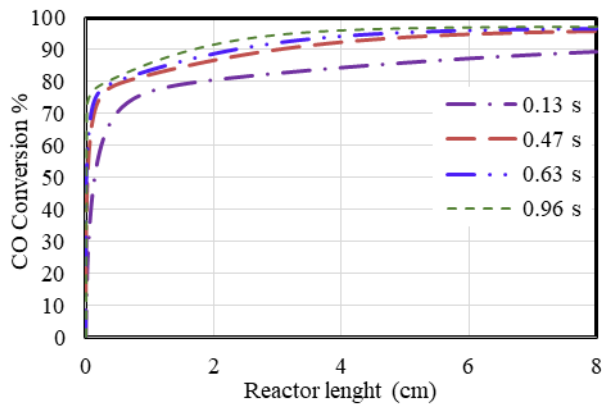


Fig. 7. CO conversion versus reactor length at fixed values of residence time.

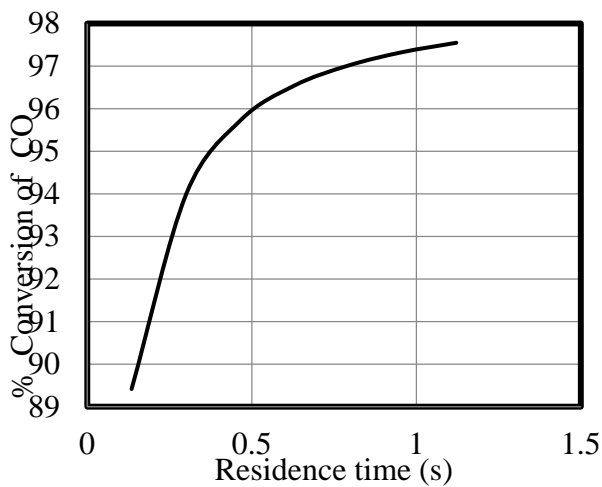


Fig. 8. Effect of residence time on CO conversion.

F. Response Surface Methodology (RSM)

The software package Minitab was used to analyse and interpret the obtained results in order to determine the optimum conditions under which the reactor can operate. Response surface methodology (RSM) in Minitab was selected owing to its excellent indications to optimise the operating conditions [20].

TABLE II: IDENTIFICATION OF AFFECTING PARAMETERS (FACTORS) USED IN THE RESPONSE SURFACE DESIGN.

Levels	Factors		
	S/C ratio	Thickness (μm)	Total retentate pressure (atm)
Level 1	1	5	2
Level 2	2.5	50	6
Level 3	4	140	8
Level 4	6	230	12

The effects of the S/C ratio, thickness (μm), and total retentate pressure (atm) on the CO conversion (response) at a

temperature of 673 K were studied. Four levels of each factor were chosen, and thus 4^3 factorial designs were simulated. Table II lists these parameters (factors) with the selected levels for each. The argon flow rate was chosen to be $3200 \text{ cm}^3/\text{min}$, as it gave the best results compared with 400 and $100 \text{ cm}^3/\text{min}$. As mentioned before, the effect of the argon flow rate of $3200 \text{ cm}^3/\text{min}$ at a thickness of $5 \mu\text{m}$ resulted in a CO conversion of approximately 98%; however, at argon flow rates of 400 and $100 \text{ cm}^3/\text{min}$ the CO conversion rates were approximately 93.7% and 87.8%, respectively. The 64 runs were performed in a random order in Minitab [17].

The best regression equation to present the data is given by (15). One of the proof of how the model fits the trend of the results is R-square and standard deviation values, which are obtained from the Minitab analysis. The high R-square value of 93.58% and small standard deviation value of 0.87 indicate that the full quadratic model is the best fit for the results obtained. Detailed Results of the regression equations are shown in Fig. 9 [17].

$$\begin{aligned}
 & \frac{(\text{Response}^\lambda - 1)}{\lambda * g^{(\lambda-1)}} \\
 &= 1.530 + (3.723 \times \text{S/C ratio}) \\
 & - (0.06265 \times \text{Thickness } (\mu\text{m})) \\
 & + (0.2783 \times \text{Total retentate pressure (atm)}) \\
 & - (0.3880 \times \text{S/Cratio} \times \text{S/Cratio}) \\
 & + (0.000130 \times \text{Thickness } (\mu\text{m}) \\
 & \times \text{Thickness } (\mu\text{m})) \\
 & + (0.003594 \times \text{S/Cratio} \times \text{Thickness } (\mu\text{m})) \\
 & - (0.0338 \times \text{S/C ratio} \\
 & \times \text{Total retentate pressure (atm)})
 \end{aligned} \tag{15}$$

where, $\lambda = 22$ and $g = 96.2198$ (the geometric mean of Response)

Response Surface Regression: Response versus S/C ratio, Thickness (μm), Total retentate					
Method					
Box-Cox transformation					
Rounded λ	22				
Estimated λ	22.3101				
95% CI for λ	(18.0876, 27.0336)				
Analysis of Variance for Transformed Response					
Source	DF	Adj SS	Adj MS	F-Value	P-Value
Model	7	618.124	88.303	116.68	0.000
Linear	3	511.239	170.413	225.17	0.000
S/C ratio	1	305.434	305.434	403.57	0.000
Thickness (μm)	1	180.536	180.536	238.54	0.000
Total retentate pressure (atm)	1	21.149	21.149	27.94	0.000
Square	2	106.756	53.378	70.53	0.000
S/C ratio*S/C ratio	1	76.773	76.773	101.44	0.000
Thickness (μm)*Thickness (μm)	1	29.983	29.983	39.62	0.000
2-Way Interaction	2	24.388	12.194	16.11	0.000
S/C ratio*Thickness (μm)	1	21.127	21.127	27.92	0.000
S/C ratio*Total retentate pressure (atm)	1	3.261	3.261	4.31	0.043
Error	56	42.382	0.757		
Total	63	660.507			
Model Summary for Transformed Response					
S	R-sq	R-sq(adj)	R-sq(pred)		
0.869987	93.58%	92.78%	91.55%		

Fig. 9. Detailed Results of the regression equations.

G. Optimum Operating Conditions

The regression model was used to determine the optimum operating conditions by using the response optimiser in Minitab, as shown in Fig. 10 [17].

The prediction of the optimiser shows the maximum CO conversion of almost 100%, which can be achieved with

conditions of: S/C ratio = 4, thickness of 5 μm , and total retentate pressure of 12 atm.

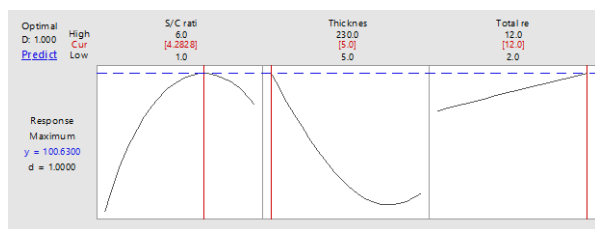


Fig. 10. Optimum conditions for response.

Another method to represent the RSM is a three-dimensional (3D) graph. Fig. [11]-[13] show the effect of each interaction on the response (CO conversion).

In Fig.11, CO conversion is plotted versus the levels of thickness and S/C ratio. The curvature of the surface plot indicates the presence of significant nonlinear relationships between the parameters. It shows that the maximum value of the CO conversion is at a moderate level of the S/C ratio (almost 4) but at a low level of thickness (5 μm). This conclusion makes sense, because as the membrane thickness decreases, the hydrogen flux through the membrane increases. However, low S/C ratios lead to less CO conversion and more carbon formation. Moreover, a high S/C ratio dilutes the hydrogen concentration on the reaction side and thus decreases its concentration, in addition to providing more energy. Therefore, a moderate S/C ratio is the better choice [17].

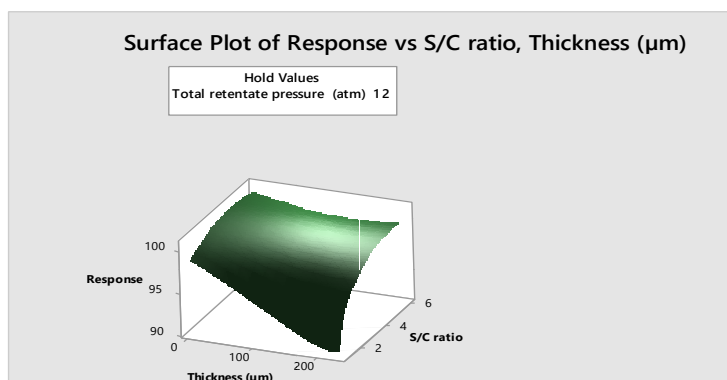


Fig. 11. Interaction effect between S/C ratio and thickness on CO conversion.

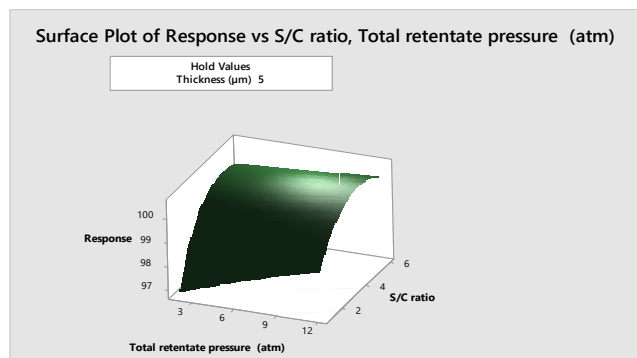


Fig. 12. Interaction effect between S/C ratio and total retentate pressure on CO conversion.

Fig. 12 illustrates the CO conversion versus the levels of S/C ratio and total retentate pressure. The 3D figure supports that the maximum value of the response is located at moderate level of S/C ratio and at high level of total retentate

pressure. Owing to an increase in the total retentate pressure, the hydrogen permeation through the membrane rises and thus the CO conversion increases [17].

The CO conversion versus the levels of thickness and total retentate pressure are shown in Fig. 13. The 3D figure supports the results obtained from Fig. 11 and 12. From the figure, it can be observed that maximum CO conversion can be achieved at a high level of total retentate pressure and a low level of the thickness, which supports all the results obtained previously [17].

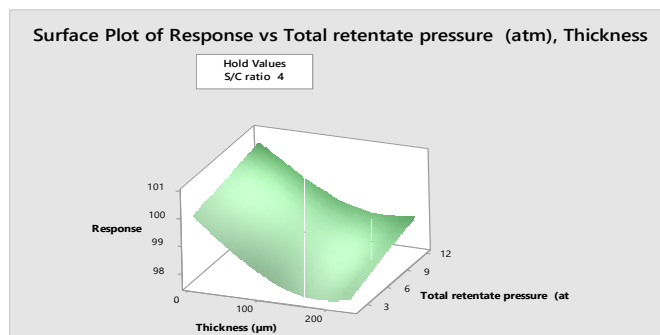


Fig. 13. Interaction effect between thickness and total retentate pressure on CO conversion.

V. CONCLUSION

In this work, the influence of palladium membrane on the WGSR under different operating conditions was investigated and optimised. Based on the results of this work, the following conclusions can be drawn:

- 1) The levels of the CO conversion with and without a membrane were examined under a temperature of 673 K, pressure of 2 atm, argon flow rate of 400 $\text{cm}^3 \cdot \text{min}^{-1}$, and S/C ratio of 1. The results revealed that the CO conversion increased from 77.5% to 93.7% after using the membrane reactor.
- 2) The effects of the S/C ratio (1–6) on the CO conversion was investigated under a temperature of 673 K, retentate pressure of 2 atm, and sweep argon flow rate of 400 $\text{cm}^3 \cdot \text{min}^{-1}$. It was found that by increasing the S/C ratio, the CO conversion increased, but at a higher S/C ratio, the hydrogen flow rate/concentration on the reaction side declined because it was diluted by the high quantity of steam, which caused a reduction in the H_2 driving force across the membrane, thereby leading to lower hydrogen recovery. Therefore, an intermediate S/C ratio of 4 was selected. The S/C ratio of 4 will reduce the energy consumed by steam generation, and it will avoid the formation of carbon.
- 3) The effect of the S/C ratio was validated by experimental results from the literature under the same operating conditions. The model predictions were in good agreement with the experimental data.
- 4) Under a temperature of 673 K, a retentate pressure of 2 atm, argon flow rates of 3200, 400, and 100 cm^3/min , and S/C ratio of 1, the effect of membrane thickness on the total CO conversion was investigated. It was noticed that as the membrane thickness decreases, the CO conversion increases. The highest CO conversion was achieved at a thickness of 5 μm . It was also observed that as the argon flow rate increases, the CO conversion

increases as well. At argon flow rates of 3200, 400, and 100 cm³/min, the CO conversions were approximately 98%, 93.7%, and 87.8%, respectively, at a thickness of 5 μm. This is because as the partial pressure of hydrogen on the permeation side declines, the level of CO conversion increases.

- 5) By increasing total pressure on the retentate side, the residence time increases and therefore the rate of reaction increases as well. This was examined under a temperature of 673 K, S/C ratio of 1, CO flow rate of 100 cm³/min, and argon flow rate of 400 cm³/min. It was found that by increasing the residence time from 0.32 to 2.69 min, CO conversion increased from 89.4% to 97.5%, respectively.
- 6) Minitab software was used to find the optimum operating conditions by using RSM analysis. The effects of the S/C ratio, thickness, and total retentate pressure at a temperature of 673 K and argon flow rate of 3200 cm³/min were studied. A total of 64 runs were performed in a random order with different combinations of factors and their corresponding responses. It was found that a nearly complete CO conversion can be achieved under an S/C ratio of 4, total retentate pressure of 12 atm, and membrane thickness of 5 μm. This supports the results obtained from the developed model.
- 7) The effect of the different parameters have been examined for a membrane reactor of small size. The aim of the future work is to examine the effect of the variables for full membrane reactor size.

REFERENCES

- [1] S. M. Hernandez-Gonzalez, "Non-catalytic production of hydrogen via reforming of diesel, hexadecane and bio-diesel for nitrogen oxides remediation," Ph.D. dissertation, University of Ohio State, United States, 2008.
- [2] M. E. Adrover, E. López, D. O. Borio, and M. N. Pedernera, "Simulation of a membrane reactor for the WGS reaction: pressure and thermal effects," *Chemical Engineering Journal*, vol. 154, no.1, pp. 196-202, Nov. 2009.
- [3] T. Maneerung, K. Hidajat, and S. Kawi, "Triple-layer catalytic hollow fiber membrane reactor for hydrogen production," *Journal of Membrane Science*, vol. 514, pp. 1-14, Sep. 2016.
- [4] L. Chibane and B. Djellouli, "Methane steam reforming reaction behaviour in a packed bed membrane reactor," *International Journal of Chemical Engineering and Applications*, vol. 2, no. 3, p. 147, Jun.
- [5] R. Ramachandran and R. K. Menon, "An overview of industrial uses of hydrogen," *International Journal of Hydrogen Energy*, vol. 23, no. 7, pp. 593-598, Jul. 1998.
- [6] J. Dufour, D. P. Serrano, J. L. Galvez, J. Moreno, and C. Garcia, "Life cycle assessment of processes for hydrogen production. Environmental feasibility and reduction of greenhouse gases emissions," *International Journal of Hydrogen Energy*, vol. 34, no. 3, pp. 1370-1376, Feb. 2009.
- [7] P. Nikolaidis and A. Poullikkas, "A comparative overview of hydrogen production processes," *Renewable and Sustainable Energy Reviews*, vol. 67, pp. 597-611, Jan. 2017.
- [8] S. Ali, M. J. Al-Marri, A. G. Abdelmoneim, A. Kumar, and M. M. Khader, "Catalytic evaluation of nickel nanoparticles in methane steam reforming," *International Journal of Hydrogen Energy*, vol. 41, no. 48, pp. 22876-22885, Dec. 2017.
- [9] O. U. Iyoha, "H₂ production in Palladium and Palladium-copper membrane reactors at 1173K in the presence of H₂S," Ph.D. dissertation, Pittsburgh, 2007.
- [10] C. M. Kalamaras and A. M. Efstathiou, "Hydrogen production technologies: Current state and future developments," in *Proc. Conference Papers in Science*, Hindawi Publishing corporation, 2013.
- [11] C. Rhodes, B. P. Williams, F. King, and G. J. Hutchings, "Promotion of Fe₃O₄/Cr₂O₃ high temperature water gas shift catalyst," *Catalysis Communications*, vol. 3, no. 8, pp. 381-384, Aug. 2002.
- [12] N. E. Amadeo and M. A. Laborde, "Hydrogen production from the low-temperature water-gas shift reaction: Kinetics and simulation of

the industrial reactor," *International Journal of Hydrogen Energy*, vol. 20, no. 12, pp. 949-956, Dec. 1995.

- [13] M. Steinberg and H. C. Cheng, "Modern and prospective technologies for hydrogen production from fossil fuels," *International Journal of Hydrogen Energy*, vol. 14, no. 11, pp. 797-820, Jan. 1989.
- [14] D. Xie, J. Yu, F. Wang, N. Zhang, W. Wang, H. Yu, F. Peng, and A. H. A. Park, "Hydrogen permeability of Pd-Ag membrane modules with porous stainless steel substrates," *International Journal of Hydrogen Energy*, vol. 36, no. 1, pp. 1014-1026, Jan. 2011.
- [15] L. D. Morpeth and M. D. Dolan, "Modelling and experimental studies of a water-gas shift catalytic membrane reactor," *Chemical Engineering Journal*, vol. 276, pp. 289-302, Sep. 2015.
- [16] S. Uemiya, N. Sato, H. Ando, and E. Kikuchi, "The water gas shift reaction assisted by a palladium membrane reactor," *Industrial & Engineering Chemistry Research*, vol. 30, no. 3, pp. 585-589, Mar. 1991.
- [17] A. A. Mourad, "Modelling and simulation of hydrogen production via water gas shift membrane reactor," M.S. thesis, Dept. Chemical and Petroleum Eng., University of United Arab Emirates, UAE, 2017.
- [18] T. L. Ward and T. Dao, "Model of hydrogen permeation behavior in palladium membranes," *Journal of Membrane Science*, vol. 153, no. 2, pp. 211-231, Feb. 1999.
- [19] R. G. Musket, "Effects of contamination on the interaction of hydrogen gas with palladium: a review," *Journal of the Less Common Metals*, vol. 45, no. 2, pp. 173-183, Mar. 1976.
- [20] D. C. Montgomery, *Design and Analysis of Experiments*, 8th ed., John Wiley & Sons, 2013.



Aya Abdel-Hamid I. Mourad awarded her BSc degree with a GPA of 3.9 (2013) and M.Sc. degree with a GPA of 3.87 (2017) in chemical engineering from the United Arab Emirates University. She was the toper of her batch. In 2013, she has worked as a graduate teaching assistant in the United Arab Emirates University. Then, she has worked as a process engineer for two years (from 2014 to 2016) in Technip France-Abu Dhabi Company, in the field of

Oil & Gas Industry. She has been involved in Front End Engineering Design (FEED) and Engineering Procurement and Construction (EPC) Projects in offshore and onshore oil & gas facilities including greenfield and Brownfield projects. She is currently working as a teaching assistant in Abu Dhabi Polytechnic. Her main research areas are, modeling and simulation of membranes for energy processes including hydrogen productions.



Nayef Ghasem is a professor of chemical engineering at the United Arab Emirates University, where he teaches mainly process modeling and simulation, natural gas processing and reactor design in chemical engineering as undergraduate courses along with other graduate and under graduate courses in chemical engineering. He has published primarily in the areas of modeling and simulation, bifurcation theory, polymer reaction engineering, advanced control and CO₂ absorption in gas-liquid membrane contactor. He has also authored principles of chemical engineering processes (CRC Press, 2012) and computer Methods in chemical engineering (CRC Press, 2009). He is a senior member of the American Institute of Chemical Engineers (AIChE).



Abdulrahman Alraeesi is an assistant professor of chemical engineering and the chair of chemical and Petroleum Engineering Department since Fall 2014, as well as the director of Emirates Center for Energy and Environment Research since Fall 2017, at the United Arab Emirates University. Dr. Alraeesi earned his Bachelor degree from UAE University, and then joined the UAE University as Teaching Assistant and earned his MSc in 2006 and PhD in chemical engineering in 2010, both from Colorado School of Mines, Golden, USA. His primary research interests are in the field of hydrogen energy, hydrogenation/dehydrogenation reactions, and metallic-based membranes separation processes. Prior to being the chair of the department, he was a member of UAE University Council during the 2011-2014 period, and a member National Faculty Development Program for four years. Abdulrahman's teaching interests include engineering thermodynamics, principles of chemical engineering processes, as well as chemical reactor design. He has been involved in program re-accreditation by ABET for both Chemical Engineering and Petroleum Engineering in 2016. He received several honors and published articles/proceedings in modeling and in hydrogen separation.